



Motion maps of glacier Viedma using Digital Image Correlation

Marcos Eduardo HARTWIG¹

¹Department of Geology, Federal University of Espírito Santo. Alto Universitário, no number, Guararema District, Alegre, state of Espírito Santo, ZIP 29500-000, Brazil.

E-mail: marcos.hartwig@ufes.br

Editor: Francisco E. Córdoba

Recibido: 31 de enero de 2023

Aceptado: 31 de julio de 2023

ABSTRACT

The Digital Image Correlation (DIC) technique allowed estimating ice displacements of several meters for the Viedma Glacier (Argentina). Different processing strategies have been adopted. The DIC with Sentinel-1 images is a very effective tool for mapping surface displacements of large-scale geological phenomena.

Keywords: mountain glacier, ice flow, radar images, displacement vector field.

RESUMEN

Mapas de desplazamiento del glaciar Viedma utilizando DIC.

La técnica de Correlación Digital de Imágenes (DIC) permitió estimar desplazamientos de hielo de varios metros para el Glaciar Viedma (Argentina). Se han probado distintas estrategias de procesamiento. El DIC con imágenes Sentinel-1 es una herramienta muy eficaz para mapear desplazamientos superficiales de fenómenos geológicos de gran escala.

Palabras clave: glaciar de montaña, flujo de hielo, imágenes de radar, campo vectorial de desplazamientos.

INTRODUCTION

There are many different techniques capable of detecting surface displacement, such as InSAR (Colesanti et al. 2006), GPS (Gili et al. 2000), LIDAR (Luzi et al. 2009), total station levelling, photogrammetry (Lucieer et al. 2014). Their use depends on the scale of the deformation phenomena, velocity and magnitude of the displacements, costs, precision and accuracy required.

Over the past two decades, there have been an increasingly use of the digital correlation method to detect surface displacements in many fields of geosciences (Van Puymbroeck et al. 2000, Strozzi et al. 2002, Casson et al. 2005, Ruiz et al. 2015, Euillades et al. 2016, Bickel et al. 2018, Caporossi et al. 2018, Morelan and Hernandez 2020). The digital corre-

lation method can use data acquired by different platforms. That is, terrestrial (fixed camera), aerial (drones and aircrafts) or orbital (satellite). The advantage of this approach is that large areas can be covered and there is no need to have any contact with targets. Moreover, costs are not disproportionate, images can be acquired with high frequency, large horizontal displacements can be detected (up to several meters) and different types of images can be employed (e.g., optical, radar, digital elevation models etc.).

In order to correlate a pair of images acquired over the same area, but at different times, they should share a common geometry (Delacourt et al. 2007). This can be achieved by orthorectification or by resampling the newest image (slave) in the geometry of the oldest image (master). In both cases, a digital elevation model is indispensable. To determine surface

displacements between a pair of images, a correlation window (subset) must be pre-defined over the master image. By using correlation functions, an equivalent window in the newest image is searched. The maximum correlation between the windows corresponds to the displacement vector. The cross-correlation coefficient is an estimator for the signal-to-noise ratio (SNR), which is a precision indicator (quality) between the subsets (Ackermann 2006).

The size of the correlation window affects the displacement accuracy. Larger windows improve the signal-to-noise ratio but reduce the displacement accuracy. Displacement accuracy equals to 1/5 of the pixel size is typical for satellite images. Displacements of up to 80 pixels have been detected by Delacourt et al. (2004) using the DIC technique. Factors such as illumination conditions (solar elevation and azimuth angles), surface state (vegetation, anthropogenic activities, thawing, erosion etc.), image noise (striping) and radiometric differences between the image pair can affect displacement calculations (Travelletti et al. 2012).

Mountain glaciers are a strategic source of water (Millan et al. 2022). They can reach hundreds of square kilometers and hundreds of meters thick and exhibit surface displacements of a few centimeters to meters per day (Aniya et al. 1996, Berthiera et al. 2005). In temperate glaciers, surface motion is due to internal ice deformation and basal sliding over bedrock (Benn and Evans 2010). At the glacier mouth, the breakage of ice (calving effect) can modify ice flow speed. Sakakibara and Sugiyama (2014) studied 28 major calving glaciers in the Southern Patagonia Icefield and concluded that on average front positions retreated 1.56 km from 1984 to 2011. Ice flow is controlled by factors such as surface slope, ice thickness and environmental temperature (Paterson 1994). Sugiyama et al. (2011) also found that fluctuations in basal meltwater pressure are an important mechanism controlling ice flow speed. Therefore, the study of ice flow in glaciers is a good indicator of climate changes which can lead to environmental impacts, such as flooding, water availability etc. (Millan et al. 2022).

In order to test the DIC, a pair of Sentinel-1 images acquired in April 2019 over the Viedma Mountain Glacier (Santa Cruz Province, southern Argentina) has been processed.

GEOLOGICAL SETTINGS

The Viedma Glacier is included in the Southern Patagonia Icefield (SPI), which is a north-south elongated icefield (48-52° S) that follows the Andean Mountain Range and reaches elevations up to 3,500 m a.s.l.. Most glaciers calve into ocean waters in the west (Chile) and proglacial lakes in the east (Ar-

gentina). Davies et al. (2020) argue that the Patagonian Ice Sheet dates back at least 35 ka years ago and has since consistently retreated.

The geology of the Viedma Glacier and its surroundings have been summarized by Giacosa et al. (2013). In the western portion and on the margins of the Viedma glacier, paleozoic rocks of low metamorphic grade (metarenites and metapelites) of the Bahía de La Lancha Formation are found in contact with Jurassic volcanic rocks of the El Quemado Complex. On the latter, small patches of Cretaceous marine sedimentary rocks (mainly sandstones, pelites and conglomerates) outcrop. Quaternary glacial deposits are found on the shores of Lake Viedma.

Structurally, the area is placed in a fault and thrust belt formed during the Tertiary through two phases of compressive deformation. It is characterized by major N-S reverse and thrust faults with eastward vergence. The Paleozoic basement also records closed folds with fold axis oblique to the regional structural trend, which would have been formed in the Gondwana orogeny.

METHODS

A pair of Sentinel-1 images acquired between 04-01-2019 and 04-01-2019 (12 days) were used. These are freely available at <https://search.asf.alaska.edu/#/>.

The SAR complex scenes were cropped, coregistered and orthorectified in SARPROZ software (Perissin et al. 2012). For the orthorectification, the SRTM-1 DEM and orbit data were used. Ground Control Points (GCPs) were not available. Orthorectified amplitude images have approximately seven meters of pixel size.

In order to retrieve horizontal displacements, the orthorectified amplitude images were correlated using the COSI-Corr algorithm implemented in IDL (Leprince et al. 2007). The statistical correlator was chosen. Different window sizes (256 to 16 pixels) have been tested. The step and search parameters were kept constant (default). The best results in terms of noise level and displacements have been achieved for the window

Table 1. Fundamental information about Sentinel-1 images used in this study.

Acquisition mode	IW – Interferometric Wide Swath
Orbit geometry	Descending
Polarization	VV
Incidence angle	32.4°
Band	C ($\lambda = 5.54$ cm)
Spatial resolution	5 x 20 m

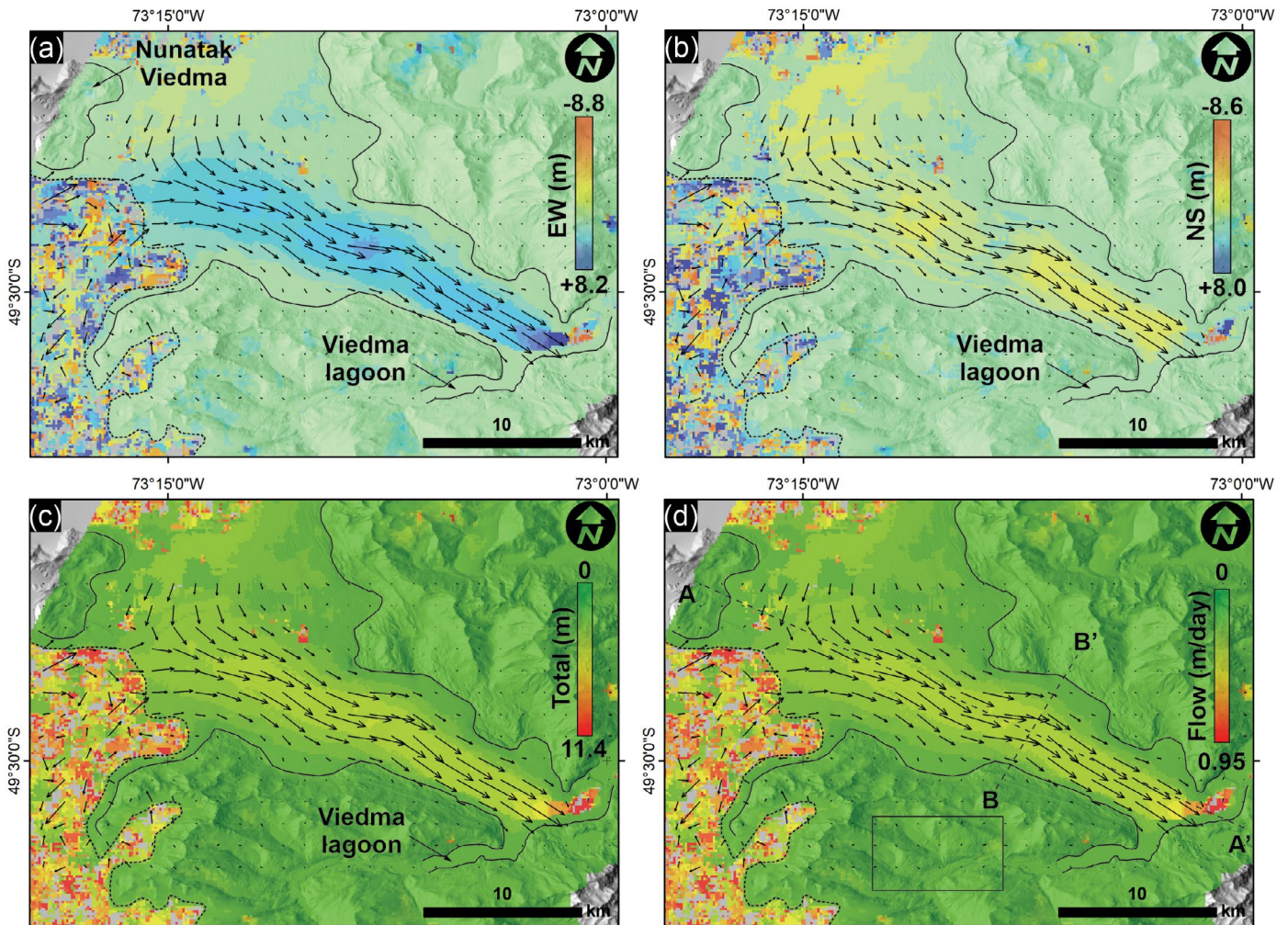


Figure 1. Motion maps for Viedma Glacier draped over a hillshaded elevation model: a) E-W; b) N-S; c) total; and d) ice flow. Arrows indicate displacement vectors. The length of the vectors indicates relative displacement. The Viedma Glacier has been outlined with the black line. The dashed line (to the left) delimits a noisy area. The rectangle refers to a selected stable area where motion uncertainties were estimated. A-A' and B-B' ice flow speed profiles.

Table 2. Estimation of the uncertainties associated with ice flow speed.

Parameters	Values (m/day)
Min.	2.25×10^{-4}
Max.	0.143
Mean	0.014
Standard deviation	0.012

size of 128 pixels. This was further processed to recover total motion and total ice flow. The first has been calculated using Pythagoras Theorem from E-W and N-S displacement maps and the second by dividing total motion by 12 days (image acquisition interval). This approach is supported by the fact that the Viedma glacier is oriented northwest-southeast. Final results have been filtered based on individual histograms to remove outliers. The uncertainties were tentatively estimated based on the displacements detected in stable areas where no motions would be expected. Positive displacement values indicate motions to the East and to the North and negative

values the opposite.

RESULTS AND DISCUSSION

The digital image correlation allowed to generate almost complete motion maps of glacier Viedma and its surroundings (Fig. 1). This figure also shows a noisy area with random motion (spurious data) where the SNR is quite low (< 0.1).

The glacier exhibits consistent displacements eastwards. The glacier head is noisy (grainy) and displacement vectors indicate that the glacier valley is fed by ice flowing from the North (highlands).

In general, EW displacements are larger than NS displacements. The largest displacements and ice velocity are found in the glacier terminus reaching up to 11.4 m and 0.95 m/day, respectively.

Figure 2 depicts ice flow profiles. Ice velocity consistently

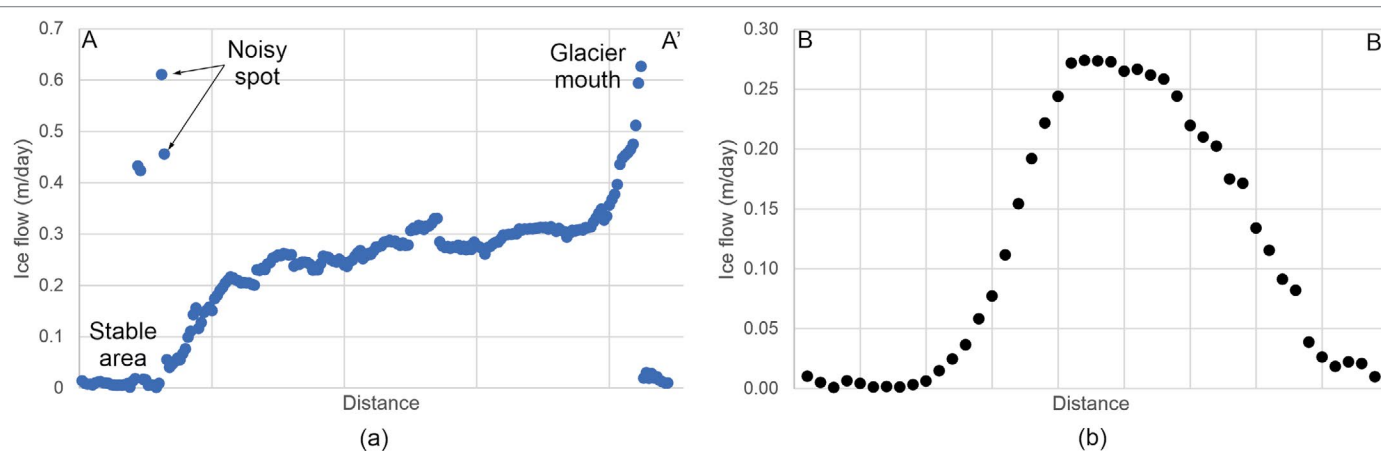


Figure 2. Longitudinal (a) and transversal (b) ice flow profiles for the Viedma Glacier. Profiles positions indicated in figure 1d.

increases downwards and inwards.

Table 2 shows basic statistics of the uncertainties associated with ice flow speed. The number of samples equals to 2,400. It can be concluded that errors are negligible over ice-free areas (0.014 ± 0.012 m/day). Thus, measurements are likely reliable because they are many orders of magnitude greater than the uncertainties.

Detected displacement field is consistent with previous studies (Muto and Furuya 2013, Riveros et al. 2013, Euillades et al. 2016, Lenzano et al. 2018, Lo Vecchio et al. 2018). It is a consensus that the average ice flow at the glacier terminus is about 2-3 m/day. These authors have used different datasets (radar and optical images from different satellites) and different processing techniques (e.g. InSAR, DIC, speckle tracking), which means that the difference between our findings and previous studies may be attributed to other factors such as: (a) the span of time between the observations (only 12 days for this study); (b) the sporadic nature of calving processes in glacier front (Muto and Furuya 2013); (c) seasonal changes, as the studies were carried out on different periods (Mouginot and Rignot 2015); and (d) ice motion is accompanied by deformation in areas with large displacements such as glacier front. Thus, surface features deform, reducing the performance of the correlation (Pitte et al. 2016).

FINAL REMARKS

The adopted approach is suitable for monitoring the dynamics of large outlet and calving glaciers, such as the ones in the South Patagonia Icefield. The method provides the total displacement and ice flow speed and direction that help understand the deformation pattern of some geological processes.

REFERENCES

- Ackermann, F. 2006. Digital image correlation: performance and potential application in photogrammetry. *The Photogrammetric Record* 11(64): 429-439.
- Aniya, M., Sato, H., Naruse, R., Skvarca, P. and Casassa, G. 1996. The use of satellite and airborne imagery to inventory outlet glaciers of the Southern Patagonia Icefield, South America. *Photogramm. Eng. Rem. S.* 62(12): 1361-1369.
- Benn, D.I. and Evans, D.J.A. 2010. *Glaciers & Glaciation*. Hodder Education. 2o. Edition, 802p., London.
- Berthiera, E., Vadonb, H., Baratoux, D., Arnaud, Y., Vincente, C., Feigl, K.L., Rémy, F. and Legrésy, B. 2005. Surface motion of mountain glaciers derived from satellite optical imagery. *Remote Sensing of Environment* 95(1): 14–28.
- Bickel, V.T., Manconi, A. and Amann, F. 2018. Quantitative assessment of digital image correlation methods to detect and monitor Surface displacements of large slope instabilities. *Remote Sensing* 10: 1-18.
- Caporossi, P., Mazzanti, P. and Bozzano, F. 2018. Digital image correlation (DIC) analysis of the 3 December 2013 Montescaglioso Landslide (Basilicata, Southern Italy): results from a multi-dataset investigation. *ISPRS International Journal of Geoinformation* 7(372): 1-25.
- Casson, B., Delacourt, C. and Allemand, P. 2005. Contribution of multi-temporal remote sensing images to characterize landslide slip surface – Application to the “La Clapière” landslide (France). *Natural Hazards and Earth System Sciences* 5: 425-437.
- Colesanti, C. and Wasowski, J. 2006. Investigating landslides with spaceborne Synthetic Aperture Radar (SAR) interferometry. *Engineering geology* 88: 173-199.
- Davies, B. J. et al. 2020. The evolution of the Patagonian Ice Sheet from 35 ka to the present day (PATICE). *Earth-Science Reviews* 103152.
- Delacourt, C., Allemand, P., Berthier, E., Raucoules, D., Casson, B., Grandjean, P., Pambrun, C. and Varel, E. 2007. Remote-sensing techniques for analysing landslide kinematics: a review. *Bulletin de Société Géologique* 178 (2): 89–100.
- Delacourt, C., Allemand, P., Casson, B. and Vadon, H. 2004. Velocity field

- of the “La Clapière” landslide measured by the correlation of aerial and QuickBird satellite images. *Geophysical Research Letters* 31: L15619.
- Euillades, L. D., Euillades, P. A., Riveros, N. C., Masiokas, M. H., Ruiz, L., Pitte, P. and Balbarani, S. 2016. Detection of glaciers displacement time-series using SAR. *Remote Sensing of Environment* 184: 188–198.
- Giacosa, R., Fracchia, D., Heredia, N. and Pereyra, F. 2013. Hoja Geológica 4972-III y 4975-IV, El Chaltén, provincia de Santa Cruz. Servicio Geológico Minero Argentino. *Boletín* 399: 89p. Buenos Aires.
- Gili, J.A., Corominas, J. and Rius, J. 2000. Using Global Positioning System techniques in landslide monitoring. *Engineering Geology* 55 (3): 167-192.
- Lenzano, M.G., Lannutti, E., Toth, C., Rivera, A. and Lenzano, L. 2018. Detecting Glacier Surface Motion by Optical Flow. *Photogrammetric Engineering & Remote Sensing* 84(1): 33–42.
- Leprince, S., Barbot, S., Ayoub, F. and Avouac, J.P. 2007. Automatic and precise ortho-rectification, co-registration and sub-pixel correlation of satellite images, application to ground deformation measurements. *IEEE Transactions on Geosciences Remote Sensing* 45(6): 1529-1558.
- Lo Vecchio, A., Lenzano, M.G., Durand, M., Lannutti, E., Bruce, R., and Lenzano, L. 2018. Estimation of surface flow speed and ice surface temperature from optical satellite imagery at Viedma Glacier, Argentina. *Global and Planetary Change* 169: 202–213.
- Lucieer, A., Jong, S.M. de and Turner, D. Mapping landslide displacements using Structure from Motion (SfM) and image correlation of multi-temporal UAV photography. 2014. *Progress in Physical Geography: Earth and Environment* 38(1): 97-116.
- Luzi, G., Noferini, L., Mecatti, D., Macaluso, G., Pieraccini, M., Atzeni, C., Schaffhauser, A., Fromm, R. and Nagler, T. 2009. Using a ground-based SAR interferometer and a terrestrial laser scanner to monitor a snow-covered slope: results from an experimental data collection in Tyrol (Austria). *IEEE Transactions on Geosciences Remote Sensing* 47(2): 382-393.
- Millan, R., Mouginot, J., Rabatel, A. and Morlighem, M. 2022. Ice velocity and thickness of the world’s glaciers. *Nature Geoscience* 15: 124–129.
- Morelan, A. E. and Hernandez, J. L. 2020. Increasing Postearthquake Field Mapping Efficiency with Optical Image Correlation. *Bulletin of the Seismological Society of America* 110(4): 1419-1426.
- Mouginot, J. and Rignot, E. 2015. Ice motion of the Patagonian Icefields of South America: 1984–2014. *Geophysical Research Letters* 42: 1441–1449.
- Muto, M. and Furuya, M. 2013. Surface velocities and ice-front positions of eight major glaciers in the Southern Patagonian Ice Field, South America, from 2002 to 2011. *Remote Sensing of Environment* 139: 50–59.
- Paterson, W. S. B. 1994. *The physics of glaciers*. Pergamon, 3rd ed.: 480p, Oxford, OX, England Tarrytown, N.Y., U.S.A.
- Perissin, D. and Wang, T. 2012. Repeat-pass SAR interferometry with partially coherent targets. *IEEE Transactions on Geosciences Remote Sensing* 50 (1): 271–280.
- Pitte, P., Berthier, E., Masiokas, M.H., Cabot, V., Ruiz, L., Ferri Hidalgo, L., Gargantini, H., and Zalazar, L. 2016. Geometric evolution of the Horcones Inferior Glacier (Mount Aconcagua, Central Andes) during the 2002–2006 surge. *Journal of Geophysical Research: Earth Surface* 121: 111–127.
- Riveros, N., Euillades, L., Euillades, P., Moreiras, S. and Balbarani, S. 2013. Offset tracking procedure applied to high resolution SAR data on Viedma Glacier, Patagonian Andes, Argentina. *Advances in Geosciences* 35: 7–13.
- Ruiz, L., Berthier, E., Masiokas, M., Pitte, P. and Villalba, R. 2015. First surface velocity maps for glaciers of Monte Tronador, North Patagonian Andes, derived from sequential Pléiades satellite images. *Journal of Glaciology* 61(229): 908–922.
- Strozzi, T., Luckman, A., Murray, T., Wegmuller, U. and Werner, C. 2002. Glacier motion estimating using SAR offset-tracking procedures. *IEEE Transactions on Geoscience and Remote Sensing* 40(11): 2384-2391.
- Sakakibara, D. and Sugiyama, S. 2014. Ice-front variations and speed changes of calving glaciers in the Southern Patagonia Icefield from 1984 to 2011. *Journal of Geophysical Research: Earth Surface* 119(11): 2541–2554.
- Sugiyama, S., Skvarca, P., Naito, N. et al. 2011. Ice speed of a calving glacier modulated by small fluctuations in basal water pressure. *Nature Geoscience* 4: 597–600.
- Travelletti, J., Delacourt, C., Allemand, P. Malet, J.P., Schmittbuhl, J., Toussaint, R. and Bastard, M. 2012. Correlation of multi-temporal ground-based optical images for landslide monitoring: Application, potential and limitations. *ISPRS Journal of Photogrammetry and Remote Sensing* 70: 39–55.
- Van Puymbroeck, N., Michel, R., Binet, R., Avouac, J.P. and Taboury, J. 2000. Measuring earthquakes from optical satellite images. *Applied Optics* 39: 3486-3494.